Synthesis and Chemical Functionalization of High Surface Area Dendrimer-Based Xerogels and Their Use as New Catalyst Supports

Joshua W. Kriesel and T. Don Tilley*

Department of Chemistry, University of California, Berkeley, Berkeley, California 94720-1460, and the Chemical Sciences Division, Lawrence Berkeley National Laboratory, 1 Cyclotron Road, Berkeley, California 94720

Received February 4, 2000

Second- and third-generation alkoxysilyl-terminated carbosilane dendrimers have been used as building blocks for the synthesis of high surface area xerogels, which were characterized by ^{29}Si CP MAS NMR spectroscopy, nitrogen adsorption/desorption porosimetry, IR spectroscopy, transmission electron microscopy (TEM), and scanning electron microscopy (SEM). Thus, the acid-catalyzed hydrolysis of $Si[CH_2CH_2CH_2Si(CH_2CH_2Si(OEt)_3)_3]_4$ (**G2-(OEt)$_{36}$**) and $Si\{CH_2CH_2CH_2Si[CH_2CH_2CH_2Si(CH_2CH_2Si(OEt)_3)_3]_3\}_4$ (**G3-(OEt)$_{108}$**) in benzene solution yielded monolithic gels. The resulting xerogels, **X-G2$_{benz}$** and **X-G3$_{benz}$**, have surface areas of 600 and 800 m^2/g, respectively. The surface area of these xerogels increase with increasing dendritic radii, suggesting that the dendrimer building blocks of **X-G2$_{benz}$** are compressed onto one another to a greater extent than the corresponding dendrimers that comprise **X-G3$_{benz}$**. The isolation of monoliths from benzene solution suggests that the hydrophobic interior of the dendrimers keeps the polymerizing species in solution. Other precursors such as TEOS, 4,4′-bis(triethoxysilyl)biphenyl, and $Si(CH_2CH_2Si(OEt)_3)_4$ (**G1-(OEt)$_{12}$**) did not yield monolithic gels after hydrolysis in benzene. Dendrimers with fewer alkoxysilyl groups at the periphery (**G2-(OEt)$_{24}$Me$_{12}$** and **G3-(OEt)$_{72}$Me$_{36}$**) were hydrolyzed in THF or benzene to materials with no appreciable surface area. After obtaining wet monolithic gels from the acid-catalyzed hydrolyses of **G2-(OEt)$_{36}$** and **G3-(OEt)$_{108}$** in benzene, postgelation processing was conducted by heating the monoliths in hot toluene for 48 h. After solvent evaporation, this procedure gave xerogels **X-G2$_{HT}$** and **X-G3$_{HT}$**, which possess surface areas of 1300 and 1000 m^2/g, respectively. These aerogel-like gels were treated with $Ti(O^iPr)_4$ to yield **X-G2$_{Ti}$** and **X-G3$_{Ti}$**. Additionally, **X-G2$_{HT}$** was treated with $Ti[OSi(O^tBu)_3]_4$ to yield **X-G2$_{Ti/Si}$**. All three gels were subsequently used as catalysts in the epoxidation of cylcohexene. These gels were shown to be very selective and significantly more active (in terms of yield and initial rate) than the Shell catalyst derived from treatment of silica with $Ti(O^iPr)_4$.

New classes of nanostructured materials with well-defined porosities have potential applications in catalysis,[1] optical devices,[2] separations,[3] and microelectronics.[4] In this context, there is increasing interest in the use of dendrimers as nanostructured building blocks for the synthesis of higher-ordered materials and nanoarchitectures.[5] Our work in this area is based on the concept that spherically shaped dendrimers might be assembled into porous networks, the structures and porosities of which should depend on the dimensions of the dendrimeric building block (i.e., its radius). For the assembly of dendrimers into porous networks, we have focused on two main strategies. One approach involves the combination of oppositely charged dendrimers possessing anionic or cationic end groups.[6] A second strategy utilizes condensation reactions which covalently link dendrimers into a network.[5c,d,7a]

We recently described the synthesis of the dendrimer-based xerogels **X-G2$_{THF}$** and **X-G3$_{THF}$** (Scheme 1).[7]

(1) (a) Corma, A. *Chem. Rev.* **1997**, *97*, 2373. (b) Ellsworth, M. W.; Gin, D. L. *Polym. News* **1999**, *24*, 331.

(2) Huo, Q.; Zhao, D.; Feng, J.; Weston, K.; Buratto, S. K.; Stucky, G. D. Schacht, S.; Schüth, F. *Adv. Mater.* **1997**, *9*, 974.

(3) (a) Feng, X.; Fryxell, G. E.; Wang, L. Q.; Kim, A. Y.; Liu, J.; Kemner K. M. *Science* **1997**, *276*, 923. (b) Mercier, L.; Pinnavaia, T. J. *Adv. Mater.* **1997**, *9*, 500.

(4) (a) Bruinsma, P. J.; Hess, N. J.; Bontha, J. R.; Liu, J.; Baskaran, S. *Mater. Res. Soc. Symp. Proc.* **1997**, *443*, 105. (b) Hedrick, J. L.; Miller, R. D.; Hawker, C. J.; Carter, K. R.; Volksen, W.; Yoon, D. Y.; Trollsas, M. *Adv. Mater.* **1998**, *10*, 1049.

(5) See for example: (a) Newkome, G. R.; Morrefield, C. N. In *Advances in Dendritic Macromolecules*; Newkome, G. R., Ed.; JAI Press: Greenwich, CT, 1994; Vol. 1, Chapter 9, and references therein. (b) Tomalia, D. A.; Naylor, A. M.; Goddard, W. A. *Angew. Chem., Int. Ed. Engl.* **1990**, *29*, 138. (c) Michalczyk, M. J.; Sharp, G. K. *J. Sol-Gel Sci. Technol.* **1997**, *8*, 541. (d) Boury, B.; Corriu, R. J. P.; Nuñez, R. *Chem. Mater.* **1998**, *10*, 1795. (e) Tomioka, N.; Takasu, D.; Takahashi, T.; Aida, T. *Angew. Chem., Int. Ed. Engl.* **1998**, *37*, 1531. (f) Coen, M. C.; Loerenz, K.; Kressler, J.; Frey, H.; Mülhaupt, R *Macromolecules* **1996**, *29*, 8069. (g) Watanabe, S.; Regen, S. L. *J. Am. Chem. Soc.* **1994**, *116*, 8855. (h) Wells, M.; Crooks, R. *J. Am. Chem. Soc.* **1996**, *118*, 3988. (i) Evenson, S.; Badyal, J. *Adv. Mater.* **1997**, *9*, 1097. (j) Liu, Y.; Bruening, M.; Bergbreiter, D.; Crooks, R. *Angew. Chem., Int. Ed. Engl.* **1997**, *36*, 2114. (k) Fan, H.; Zhou, Y.; López, G. *Adv. Mater.* **1997**, *9*, 728. (l) Newkome, G.; Güther, R.; Moorefield, C.; Cardullo, F.; Echegoyen, L.; Pérez-Cordero, E.; Luftmann, H. *Angew. Chem., Int. Ed. Engl.* **1995**, *34*, 2023. (m) Tsukruk, V. V. *Adv. Mater.* **1998**, *10*, 253 and references therein.

(6) (a) Kriesel, J.; König, S.; Freitas, M. A.; Marshall, A. G.; Leary, J. A.; Tilley, T. D. *J. Am. Chem. Soc.* **1998**, *120*, 12207.

10.1021/cm000098g CCC: $19.00
Published on Web 03/24/2000

Scheme 1

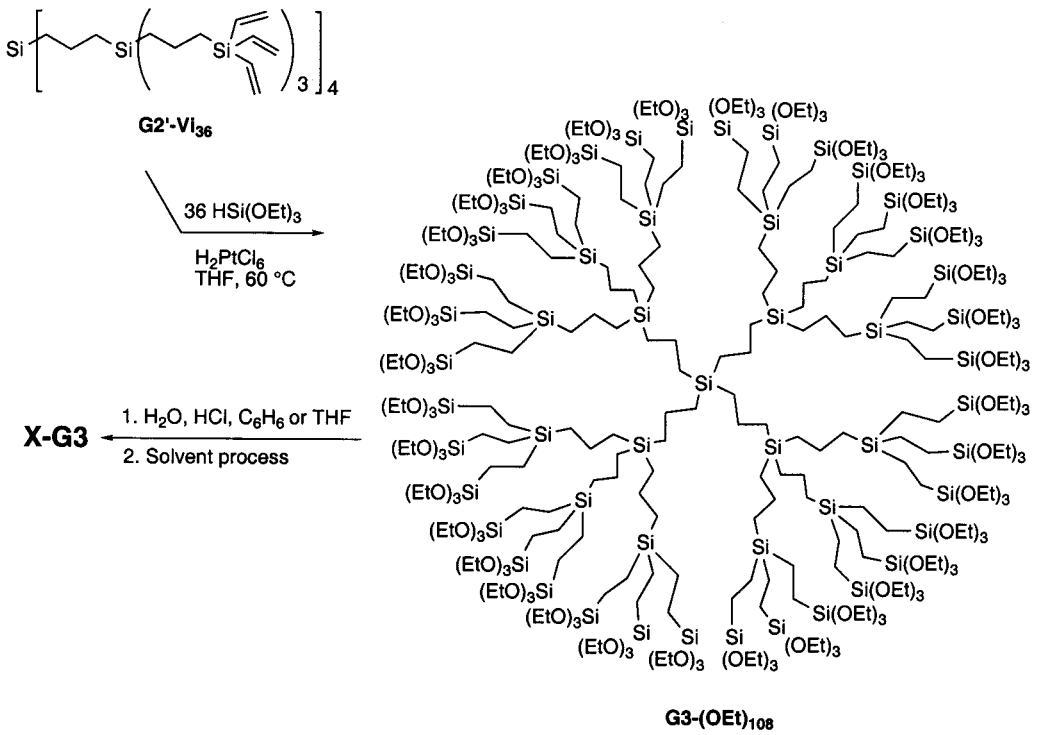

These relatively high surface area materials (325 and 490 $m^2\ g^{-1}$, respectively) were prepared by the acid-catalyzed hydrolysis of second- and third-generation alkoxysilyl-terminated carbosilane dendrimers (**G2-(OEt)$_{36}$** and **G3-(OEt)$_{108}$**) in THF solution. The resulting xerogels exhibit a high degree of microporosity, apparently because pores in the "wet" gel undergo considerable collapse during removal of the polar THF solvent. In an attempt to minimize this pore collapse and obtain predominantly mesoscopic pores, we investigated alternative processing conditions. Here we report the use of nonpolar solvents and high-temperature drying conditions which allow synthesis of mesoporous, dendrimer-based materials with remarkably high surface areas (600−1300 $m^2\ g^{-1}$). These materials maintain a high degree of Si−OH functionalization, which allows chemical modification of the gel network. This latter feature has been used to prepare titanium-supported catalysts which exhibit very high selectivities and activities for the epoxidation of cyclohexene.

Results and Discussion

Synthesis and Characterization of Dendrimer-Based Xerogels. Hydrolyses of **G2-(OEt)$_{36}$** and **G3-(OEt)$_{108}$** were conducted in benzene solution (2.5 M in OEt groups) with small quantities of 1 N HCl.[8] The heterogeneous sol solutions were stirred for 20 min, transferred to polyethylene bottles, and allowed to gel for 7 days. Hard, clear homogeneous monoliths were subsequently obtained and washed in a fine-fritted Büchner funnel with copious amounts of benzene. The monoliths were then air-dried for several days, powdered, and then dried under high vacuum at 100 °C overnight to yield **X-G2$_{benz}$** and **X-G3$_{benz}$**, respectively.

Although the use of nonpolar solvents in sol−gel chemistry is desirable from the standpoint of minimizing pore collapse upon drying of the wet gel, they are, in fact, rarely used.[9] Presumably this is due to the limited solubility of water in these media, which is expected to result in heterogeneous sol solutions which would give particulate, rather than monolithic, materials. Thus, it is interesting that the hydrolyses of **G2-(OEt)$_{36}$** and **G3-(OEt)$_{108}$** in benzene produce monoliths.

BET analyses of these gels revealed that their surface areas, average pore sizes, and pore volumes increase with increasing dendrimer generation (Table 1). This finding was somewhat unexpected based on what is known about the condensation of silica particles, for which surface areas generally decrease as the condensing particle size increases.[10] Note that this trend was previously observed for the xerogels **X-G2$_{THF}$** and **X-G3$_{THF}$**, with **X-G2$_{THF}$** having the lower surface area (Table 1).[7a] To explain this apparent anomaly, we suggested that the dendrimers exhibit some degree of compressibility and, in particular, that **G2-(OEt)$_{36}$** is more deformable than **G3-(OEt)$_{108}$**. Thus, the dendrimers that comprise **X-G2$_{THF}$** are probably compressed onto one another, thereby leaving a lower surface area than one would expect for the packing of hard spheres. Apparently, this factor is still operative in xerogels **X-G2$_{benz}$** and **X-G3$_{benz}$**. The much larger surface areas of **X-G2$_{benz}$** and **X-G3$_{benz}$**, as compared to the analogous

(7) (a) Kriesel, J.; Tilley, T. D. *Chem. Mater.* **1999**, *11*, 1190. (b) The nomenclature for the xerogels denotes the method of solvent removal from the gel (**X** = xerogel), generation of the dendrimer building block (e.g., **G2**) and the last solvent used in the isolation (e.g., THF). Thus, **X-G2$_{THF}$** denotes a xerogel made from a second-generation dendrimer and isolated from THF.

(8) For general synthetic methodology see ref 7a.

(9) Brinker, C. J.; Scherer, G. W. *Sol−Gel Science: The Physics and Chemistry of Sol−Gel Processing*; Academic Press: San Diego, 1990.

(10) (a) Lecloux, A. J.; Bronckart, J.; Noville, F.; Dodet, C.; Marchot, P.; Pirard, J. P. *Colloids Surf.* **1986**, *19*, 359. (b) Iler, R. K. *The Chemistry of Silica*; John Wiley and Sons: New York, 1979.

Table 1. Nitrogen Porosimetry Data for the Xerogels

xerogel	BET surface area ($m^{2/g}$)	total pore volume (cc/g)	average pore radius (Å)[a] (2·V/A)	average pore radius (Å)[b] (BJH)	micropore area (m^2/g)
X-G2$_{THF}$	325	0.21	13	10[c]	227
X-G3$_{THF}$	490	0.33	14	10[c]	272
X-G2$_{benz}$	616	0.36	15	13	164
X-G3$_{benz}$	806	0.70	17	13	102
X-G2$_{HT}$	1336	2.08	31	218	0
X-G3$_{HT}$	1006	0.96	19	46	46
X-G2$_{Ti}$	637	1.13	35	148	0
X-G3$_{Ti}$	484	0.53	22	47	0
X-G2$_{Ti/Si}$	764	1.18	31	101	0
X$_{TEOS}$	416	0.27	13	46	257
X$_{biphen}$	47	0.03	11	10[c]	28
microporous silica[33]	496	0.31	16		
silica aerogel[9,19]	858	0.82	19	5−250	
Shell catalyst	187	0.69	73	442	17

[a] Average pore radii were calculated using 2(pore volume)/surface area. [b] The BJH average pore radii were determined from the global maximum of the adsorption pore size distribution. [c] Although the pore size distribution suggests that there are a large number of pores with radii < 10 Å, the BJH model cannot account for this "microporosity." Therefore, these values may not be the true global maximum of the pore size distribution.

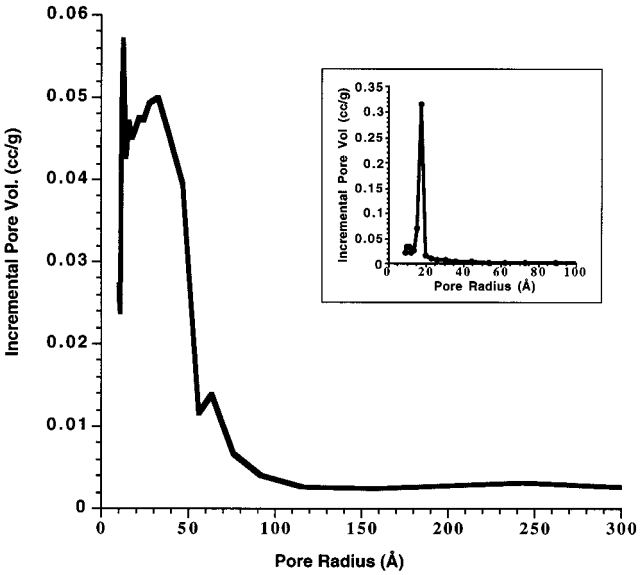

Figure 1. The differential pore size distribution (incremental pore volume (cc/g) vs pore radius (Å) for the gel derived from dendrimer **G3-(OEt)$_{108}$** (**X-G3$_{benz}$**) using the *adsorption* isotherm data. The pore size distribution calculated from the *desorption* branch of the isotherm is shown in the inset.

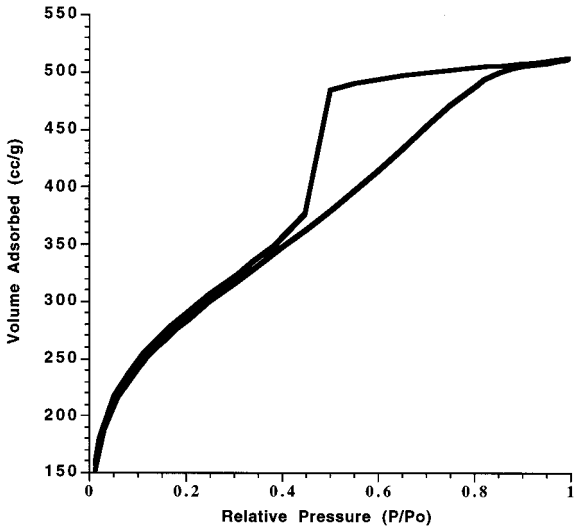

Figure 2. The nitrogen adsorption/desorption isotherm for the xerogel derived from **G3-(OEt)$_{108}$** (**X-G3$_{benz}$**).

xerogels made in THF, is probably due to a reduction in the degree of pore collapse usually attributed to the use of a nonpolar solvents.[9,11] For example, the surface area of **X-G3$_{benz}$** is 806 m^2/g, as compared to 490 m^2/g for **X-G3$_{THF}$**.

The nitrogen adsorption/desorption isotherms for **X-G2$_{benz}$** and **X-G3$_{benz}$** reveal the presence of relatively large pores having radii of ∼10−80 Å (average pore radii of ∼13 Å for both materials). An analysis of the pore size distributions, using the Barrett−Joyner−Halenda (BJH)[12] and t-plot methods[13] suggests that the micropore contribution to the total surface area is relatively minor, and smaller than the micropore contributions observed for **X-G2$_{THF}$** and **X-G3$_{THF}$** (Table 1). Further, comparison of the pore size distributions calculated from the adsorption and desorption portions of the individual isotherms indicate a geometrical pore model of narrow necks as entrances to wider cavities (see Figure 1).[9,14,15] The isotherm for **X-G3$_{benz}$**, shown in Figure 2, is reminiscent of a type H2 hysteresis[14] (type E in the older literature[12]). This type of hysteresis has been attributed to ink-bottle type pores, although it is now recognized that this may be an oversimplification of the actual pore structure.[14]

To determine whether high surface area materials and monolithic products could also be obtained from simpler molecular precursors, the hydrolyses of $Si(OEt)_4$ (TEOS) and $(EtO)_3SiC_6H_4C_6H_4Si(OEt)_3$ (4,4′-bis(triethoxysilyl)biphenyl)[16] in benzene solution were investigated. The hydrolyses of these species in benzene at

(11) Terry, K. W.; Lugmair, C. G.; Tilley, T. D. *J. Am. Chem. Soc.* **1997**, *119*, 9745.
(12) Barrett, E. P.; Joyner, L. G.; Hakebda, P. P. *J. Am. Chem. Soc.* **1951**, *73*, 373.
(13) Lippens, B. C.; de Boer, J. H. *J. Catal.* **1965**, *4*, 319.
(14) Sing, K. S. W.; Everett, D. H.; Haul, R. A. W.; Moscou, L.; Pierotti, R. A.; Rouqerol, J.; Siemieniewska, T. *Pure Appl. Chem.* **1985**, *57*, 603.
(15) (a) Lowell, S.; Shields, J. E. *Powder Surface Area and Porosity*, 2nd ed.; Chapman and Hall: London, 1984. (b) Gregg, S. J.; Sing, K. S. W. *Adsorption, Surface Area and Porosity*, 2nd ed.; Academic Press Inc.: London, 1982.
(16) Shea, K. J.; Loy, D. A.; Webster, O. *J. Am. Chem. Soc.* **1992**, *114*, 6700.

the same ethoxy group concentration (2.5 M) resulted in no gelation after 4 weeks. At higher concentration (3.5 M in OEt groups), the hydrolysis of TEOS led to a particulate silica gel ($\mathbf{X_{TEOS}}$) over 6 days. The relatively small BET surface area (416 m^2/g) and pore volume of $\mathbf{X_{TEOS}}$ (Table 1) is similar to that of a microporous silica. Hydrolysis of 4,4′-bis(triethoxysilyl)biphenyl (at 3.5 M in OEt groups) in benzene yielded a particulate material ($\mathbf{X_{biphen}}$) only after 3 weeks in a closed container, and the BET surface area of this material is 47 m^2/g (Table 1). Therefore, the hydrolyses of TEOS and 4,4′-bis(triethoxysilyl)biphenyl in benzene did not produce monolithic gels. This finding implies that the hydrolyzed molecular species do not polymerize into a highly extended network, and instead the growing clusters eventually become insoluble in benzene and precipitate out of solution. Moreover, the precipitation of solid particles from solution in this way is expected to yield a relatively dense material,[17] which should have a lower surface area than a polymeric (monolithic) gel.

It is important to note that small molecules such as TEOS and 1,4-bis(triethoxysilyl)benzene can be hydrolyzed to very high surface area materials under conditions different from those discussed above (nonpolar solvents and acid catalysis). For example, Corriu has prepared high surface area xerogels from 1,4-bis(triethoxysilyl)benzene via a base-catalyzed hydrolysis in THF,[18] and Shea has employed both acid- and based-catalyzed hydrolyses to obtain hybrid organic−inorganic materials with similar properties.[16]

The results described above indicate that the structure of the alkoxysilyl precursor compound is very important in determining the ultimate properties for the hydrolyzed material. To further explore this apparent structure−property relationship, we examined the hydrolysis of $Si[CH_2CH_2Si(OEt)_3]_4$, **G1-(OEt)$_{12}$**. The hydrolysis of this species in benzene, using a protocol identical to that used for the syntheses of **X-G2$_{benz}$** and **X-G3$_{benz}$**, did not give a monolithic gel. Instead, only a small amount of solid precipitate was obtained after several weeks. Similar results have been reported for the related species $Si[CH_2CH_2CH_2Si(OEt)_3]_4$[5c] and $Si[CH_2CH_2Si(OMe)_3]_4$.[5d] The compound $Si[CH_2CH_2CH_2Si(OEt)_3]_4$ was reported to hydrolyze in THF to a "low surface area material",[5c] and $Si[CH_2CH_2Si(OMe)_3]_4$ did not gel after base-catalyzed hydrolyses in EtOH, THF, or acetone. The latter result was attributed to intramolecular condensation.[5d] Apparently, intermolecular condensation does not occur to a great enough extent to yield an extended network, and hence, a gel. Clearly, both the precursor structure and the number of end groups play a role in determining the gelation behavior and the ultimate properties of the material. These results suggest that an important factor controlling the gelation behavior for alkoxysilyl-terminated species is the number of hydrolyzable groups per monomer.

To further elucidate the relationship between the number of hydrolyzable groups and the gelation behavior, we synthesized generational analogues to **G2-(OEt)$_{36}$** and **G3-(OEt)$_{108}$** possessing fewer alkoxy groups per silicon center. Thus, **G2-(OEt)$_{24}$Me$_{12}$** and **G3-(OEt)$_{72}$Me$_{36}$** were prepared by hydrosilylation of the appropriate vinyl-terminated dendrimers with $HSiMe(OEt)_2$. Hydrolyses of these species, employing the conditions described above for **X-G2$_{THF}$** and **X-G2$_{benz}$**, yielded soft monolithic products after ∼10−14 days. Desiccation of the wet monoliths yielded xerogels **X-G2Me$_{THF}$**, **X-G2Me$_{benz}$**, **X-G3Me$_{THF}$**, and **X-G3Me$_{benz}$**. All four of these materials had no detectable surface area, as determined by BET analysis. Apparently, fewer reactive groups per unit volume results in longer gel times and gels with less structural rigidity.

Table 2. ^{29}Si CP MAS NMR Spectroscopic Data for the Xerogels

xerogel	T^1 (%)	T^2 (%)	T^3 (%)	degree of condensation
X-G2$_{THF}$	5.6	83.8	10.6	68.3
X-G3$_{THF}$	5.0	85.9	9.1	68.0
X-G2$_{benz}$	8.2	67.3	24.6	72.1
X-G3$_{benz}$	8.6	68.5	22.9	71.4
X-G2$_{HT}$	6.1	57.4	36.5	76.8
X-G3$_{HT}$	6.8	74.6	18.6	70.6
X-G2$_{Ti}$	0	58.0	42.0	
X-G3$_{Ti}$	0	26.6	73.4	
X-G2$_{Ti/Si}$	0	54.0	46.0	

Solid-state ^{29}Si CP-MAS NMR spectroscopy was employed to determine the degree of condensation in **X-G2$_{benz}$** and **X-G3$_{benz}$**. The silicon centers at the terminus of the condensed dendrimers are designated T^1, T^2, and T^3 denoting one, two, or three Si−O−Si linkages, respectively. By deconvolution of the individual T^n resonances, an estimate (± 10%) of the degree of condensation in the gels was made.[16,19] This method for estimating the relative number of different silicon centers and quantifying the degree of condensation is thought to be reasonably accurate for assessing trends in related materials.[16] Thus, it is instructive to compare NMR data for different xerogels composed of dendrimers of the same generation (Table 2). Xerogels **X-G2$_{benz}$** and **X-G3$_{benz}$** have degrees of condensation higher than the corresponding xerogels produced in THF. Furthermore, there are significantly more fully condensed silicon centers (T^3) in the xerogels made from benzene. This is perhaps somewhat surprising due to the relative solubilities of H_2O in THF and benzene, but suggests that the polymerizing dendrimeric species remain extremely soluble in benzene solution, thereby allowing a high degree of condensation.

Although the surface areas of **X-G2$_{benz}$** and **X-G3$_{benz}$** are quite high, there is undoubtedly substantial residual EtOH and H_2O entrapped in the pore structures of the isolated xerogels. This was confirmed by TGA analyses of **X-G2$_{benz}$** and **X-G3$_{benz}$**, which revealed gradual weight losses of ∼15% between 80 and 130 °C. These residual byproducts arise from the condensation polymerization and probably contribute significantly to pore collapse. In an effort to flush the EtOH and H_2O out of the gels, the wet solid monoliths obtained from hydrolyses of **G2-(OEt)$_{36}$** and **G3-(OEt)$_{108}$** in benzene were heated at 100 °C for 48 h in toluene. With this solvent processing protocol, gels **X-G2$_{HT}$** and **X-G3$_{HT}$** were obtained as fluffy, off-white powders.

(17) Pierre, A. C. *Introduction to Sol−Gel Processing*; Kluwer Academic Publishers: Boston, 1998.

(18) Cerveau, G.; Corriu, R. J. P.; Framery, E. *Chem. Commun.* **1999**, 2081.

(19) Glaser, R. H.; Wilkes, G. L.; Bronnimann, C. E. *J. Non-Cryst. Solids* **1989**, *113*, 73.

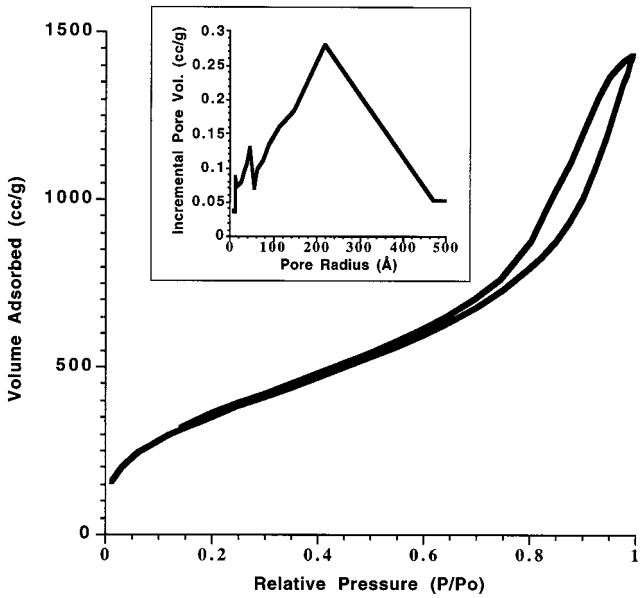

Figure 3. The adsorption/desorption isotherm for the gel derived from dendrimer **G2-(OEt)$_{36}$** after hydrolysis in benzene and solvent processing in hot toluene (**X-G2$_{HT}$**). The differential pore size distribution (incremental pore volume vs pore radius) derived from the *adsorption* isotherm data for this gel is shown in the inset.

Analyses of **X-G2$_{HT}$** and **X-G3$_{HT}$** by nitrogen adsorption/desorption porosimetry revealed that the surface areas and pore volumes of these xerogels are remarkably high, and in fact similar in magnitude to what has been observed for silica aerogels (Table 1).[9,20] Indeed, the BET isotherm for **X-G2$_{HT}$** (Figure 3) is similar in shape and volume of adsorbed gas to what one might expect for an aerogel. The isotherm loop for **X-G2$_{HT}$** represents a type H3 hysteresis,[9,20] which has been attributed to the tenuous assembly of particles that define slit-shaped pores.[15] Further, the pore size distribution derived from the adsorption branch of the isotherm exhibits a maximum pore radius of 220 Å (Figure 3). The nitrogen adsorption/desorption isotherm for **X-G3$_{HT}$** also has the approximate shape associated with an H3-type loop; however, it also contains some H2-type character, indicating that the pore structure is more complex. The pore size distribution for **X-G3$_{HT}$**, as determined from the adsorption branch of the isotherm, is bimodal with a global maximum at 46 Å. However, it is important to note that nitrogen adsorption/desorption porosimetry has been shown to be inaccurate for determining pore volumes and sizes in aerogels.[21] Thus, to the extent that **X-G2$_{HT}$** and **X-G3$_{HT}$** are aerogel-like, the corresponding pore size data may be misleading.

From the BET surface area data, it seems that the hot toluene washing protocol for **X-G2$_{HT}$** and **X-G3$_{HT}$** effectively removes substantial quantities of H_2O and EtOH from the wet gels, thus minimizing the capillary forces that contribute to pore collapse. Since the surface area trend with respect to dendrimer generation now occurs in a manner consistent with that expected for the packing of spheres, the extent to which the dendrimers are compressed onto one another has apparently been reduced. However, the ^{29}Si CP-MAS NMR spectroscopic data for **X-G2$_{HT}$** indicates that there has also been further condensation during this processing of the wet gel (Table 2). In particular, comparison of the T^3 values for **X-G2$_{benz}$** and **X-G2$_{HT}$** reveals a nearly 12% increase in the number of fully condensed silicon centers upon high-temperature solvent processing. Since **X-G2$_{HT}$** and **X-G3$_{HT}$** were solvent-processed after gelation, it appears that subsequent condensations occur within a dendrimer building block.

TEM micrographs of all the xerogels made in benzene reveal the random packing of approximately spherical particles, and aggregates of spheres. Further, the morphologies of these materials are relatively open as compared to those for **X-G2$_{THF}$** and **X-G3$_{THF}$**.[7a] However, the pore sizes of **X-G2$_{HT}$** and **X-G3$_{HT}$** (as determined by TEM) are inconsistent with those obtained from BET data, probably due to the observed beam damage for these highly open structures. Thus, we employed scanning electron microscopy (SEM) to compare the surface morphology of the xerogels made in THF with those made from benzene with the hot toluene wash. The SEM studies for **X-G2$_{THF}$** revealed a smooth gellike texture consistent with a material containing substantial *microporosity* (Figure 4a).[22] Conversely, the SEM micrographs for **X-G2$_{HT}$** revealed a very rough texture with globular aggregates (Figure 4b). The texture of this material is reminiscent of inorganic−organic hybrid aerogels made by Shea[23] and of dendrimer-based aerogels made by super critical CO_2 extraction.[24] Similar results were observed for **X-G3$_{THF}$** vs **X-G3$_{HT}$**.

Stability and Chemical Functionalization of the Xerogels. To compare the surface properties of the dendrimer-based xerogels with those of more conventional silica-based materials, we estimated the number of surface hydroxyl groups in the xerogels. From ^{29}Si CP MAS NMR spectra, we estimate the total number of free Si−OH groups in **X-G2$_{HT}$** and **X-G3$_{HT}$** as 6.7 and 7.3 mmol/g, respectively. These values can be converted to a "hydroxyl surface coverage" via their respective surface areas. Thus, **X-G2$_{HT}$** and **X-G3$_{HT}$** have hydroxyl surface coverages of 3.0 and 4.4 OH/nm^2, respectively. Typical silica aerogels have surface hydroxyl coverages of 5.0−5.7 OH/nm^2, whereas partially dehydroxylated silicas normally contain 1.2−2.6 OH/nm^2.[9,25]

Since **X-G2$_{HT}$** has a high surface area and significant Si−OH coverage, we were motivated to further evaluate this material as a catalyst support. Therefore, we first examined the stability of **X-G2$_{HT}$** by heating it at reflux in a variety of solvents, and subsequently measuring the BET surface area of the isolated gel. We found that there was no loss in surface area or pore volume after heating **X-G2$_{HT}$** at reflux for 48 h in C_6H_6, THF or H_2O.

Before using the dendrimer-based xerogels as catalyst supports, more information was accumulated on the

(20) Brinker, C. J.; Keefer, K. D.; Schaefer, D. W.; Ashley, C. S. *J. Non-Cryst. Solids* **1982**, *48*, 47.

(21) The pore volumes and pore size distributions for aerogels have been shown to be inaccurate: Scherer, G. W.; Smith, D. M.; Stein, D. *J. Non-Cryst. Solids* **1995**, *186*, 309.

(22) See for example: (a) Loy, D. A.; Carpenter, J. P.; Yamanaka, S. A.; McClain, M. D.; Greaves, J.; Hobson S.; Shea, K. J. *Chem. Mater.* **1998**, *10*, 4129. (b) Tamaki, R.; Chujo, Y.; Kuraoka, K.; Yazawa, T. *J. Mater Chem.* **1999**, *9*, 1741.

(23) See for example: (a) Loy, D. A.; Jamison, G. M.; Baugher, B. M.; Myers, S. A.; Assink, R. A.; Shea, K. J. *Chem. Mater.* **1996**, *8*, 656. (b) Loy, D. A.; Shea, K. J. *Chem. Rev.* **1995**, *95*, 1431.

(24) Kriesel, J. W.; Tilley, T. D. Unpublished results.

(25) Morrow, B. A. *Stud. Surf. Sci. Catal.* **1990**, *57A*, 161.

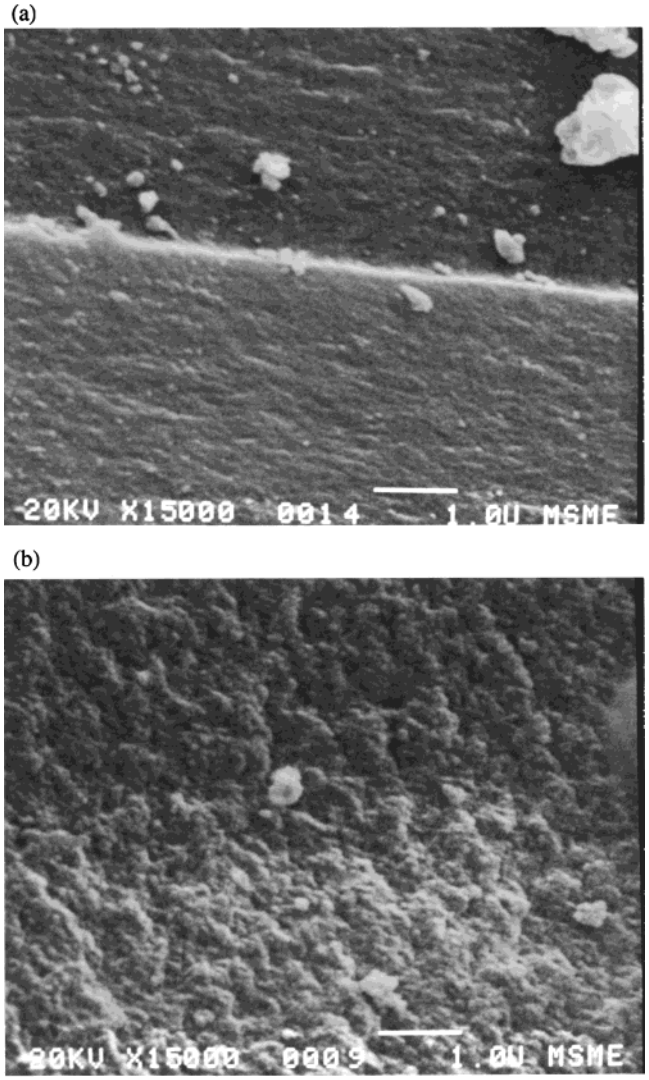

Figure 4. SEM micrographs of **X-G2$_{THF}$** showing a smooth gel-like texture (a) and **X-G2$_{HT}$** showing a rough texture reminiscent of an aerogel (b).

Table 3. Quantity of Si−OH on the Xerogels that Reacted Chemically with the Soluble Reagent, As Determined by NMR Spectroscopy (See Experimental Section)[a]

xerogel	$ClSiMe_2H$	$ClSiMe_3$	$ClSi^tBu_2Me$	$Ti(O^iPr)_4$
X-G2$_{HT}$	10.2	6.8	2.3	3.6
X-G3$_{HT}$	4.6	3.2	2.2	1.3

accessibility of the pores to molecular species that might potentially graft to the gel surface. Thus, we examined the uptake of various chlorosilanes (Me_2SiHCl, Me_3SiCl, and $Me_2{}^tBuSiCl$) by NMR spectroscopy in the presence of **X-G2$_{HT}$** and **X-G3$_{HT}$**. These experiments allowed us to quantify the amount of chlorosilane that covalently bonded to 1 g of the xerogel. As expected, the smaller chlorosilanes reacted more extensively with the gel (Table 3). In the case of **X-G2$_{HT}$**, with only ~6.7 mmol of hydroxyl groups per gram of gel, 6.8 mmol of Me_3SiCl, and 10.2 mmol of Me_2SiHCl were consumed in the respective grafting reactions. This may be due to the release of HCl in the initial silylation reaction, which can cleave Si−O−Si bonds to produce additional silanol functionalities. Thus, these types of experiments seem to be of limited use in quantifying the number of −OH sites initially present.

Epoxidation Catalysis. Recently, Ti-containing silica materials have received considerable attention as catalysts. Their applications in catalysis have involved the selective oxidation of olefins, acid-catalyzed isomerizations and the oxidation of saturated hydrocarbons.[26] Several of the Ti-based epoxidation catalysts have been synthesized by treatment of conventional silica gels with soluble titanium molecular precursors, such as $Ti(O^iPr)_4$ and $Ti[OSi(O^tBu)_3]_4$.[27] Initially, we envisioned the sol−gel-derived dendrimer-based gels as being ideal candidates for catalyst supports due to their high surface areas, ease of surface functionalization, and tunable porosities. Thus, given that **X-G2$_{HT}$** and **X-G3$_{HT}$** have very high surface areas and readily undergo chemical modification, we investigated their performance as supports for titanium in the catalytic epoxidation of olefins.

Treatment of the dendrimer-based xerogels with an excess of $Ti(O^iPr)_4$ in refluxing toluene for 48 h produced the titanium-containing materials **X-G2$_{Ti}$** and **X-G3$_{Ti}$**, after extensive washing with toluene and hexanes. Ti complexation onto the gels was confirmed by elemental analyses, which revealed Ti contents of 7.91 and 7.61% for **X-G2$_{Ti}$** and **X-G3$_{Ti}$**, respectively. Similarly, **X-G2$_{HT}$** was heated at reflux for 2 days in a toluene solution of $Ti[OSi(O^tBu)_3]_4$, and subsequent washing with copious amounts of hexanes yielded **X-G2$_{Ti/Si}$**. The elemental analysis of this gel revealed a Ti content of 3.27%. The Ti content in **G2$_{Ti/Si}$** is probably lower than that of the corresponding gel grafted with $Ti(O^iPr)_4$ due to the relatively greater steric bulk of $Ti[OSi(O^tBu)_3]_4$.

All three xerogels were further analyzed by BET analysis, which revealed reductions in the pore volumes and surface areas relative to the ungrafted materials (see Table 1). Additionally, the general shapes of the isotherms for **X-G2$_{Ti}$**, **X-G3$_{Ti}$**, and **X-G2$_{Ti/Si}$** are virtually identical to those of the ungrafted gels, indicating that the integrity of the pore structure is preserved through the grafting procedure. ^{29}Si CP-MAS NMR spectroscopy of **G2$_{Ti}$**, **X-G3$_{Ti}$**, and **X-G2$_{Ti/Si}$** revealed the absence of T^1 resonances, indicating that all of the $-Si(OH)_2$ sites had reacted. The reaction of $Ti[OSi(O^tBu)_3]_4$ with **X-G2$_{HT}$** was also monitored by NMR spectroscopy, which revealed that titanium binding resulted in production of HO^tBu and $HOSi(O^tBu)_3$, in a 3:1 ratio. Further, the ^{29}Si CP-MAS NMR spectrum of **X-G2$_{Ti/Si}$** contained a small peak at ca. −100 ppm attributed to the siloxide silicon atoms of the grafted Ti complexes ($TiOSi(O^tBu)_3$ or $TiOSi(O^tBu)_2O$ groups). No calcination of the Ti-grafted dendrimer-based gels was performed prior to their use as catalysts. Indeed, catalysts derived from the grafting of $Ti(O^iPr)_4$ onto silica (without calcination) have been shown to be highly efficient for olefin epoxidation.[28]

(26) See, for example: (a) Davis, R. J.; Liu, Z. *Chem. Mater.* **1997**, *9*, 2311. (b) Klein, S.; Thorimbert, S.; Maier, W. F. *J. Catal.* **1996**, *163*, 476. (c) Murugavel, R.; Roesky, H. W. *Angew. Chem., Int. Ed. Engl.* **1997**, *36*, 477.

(27) See, for example: (a) Cativiela, C.; Fraile, J. M.; García, J. I.; Mayoral, J. A. *J. Mol. Catal.* **1996**, *112*, 259. (b) Hutter, R.; Mallat, T.; Baiker, A. *J. Catal.* **1995**, *153*, 177. (c) Maschmeyer, T.; Rey, F. Sankar, G.; Thomas, J. M. *Nature* **1995**, *378*, 159. (d) Coles, M. C.; Lugmair, C. G.; Terry, K. W.; Tilley, T. D. *Chem. Mater.* **1999**, *11*, 122. (e) Fraile, J. M.; García, J. I.; Mayoral, J. A.; Proeitti, M. G.; Sánchez, M. C. *J. Phys. Chem.* **1996**, *100*, 19484.

(28) Fraile, J. M.; García, J. I.; Mayoral, J. A.; de Mènorval, L. C.; Rachdi, F. *J. Chem. Soc., Chem. Commun.* **1995**, 539.

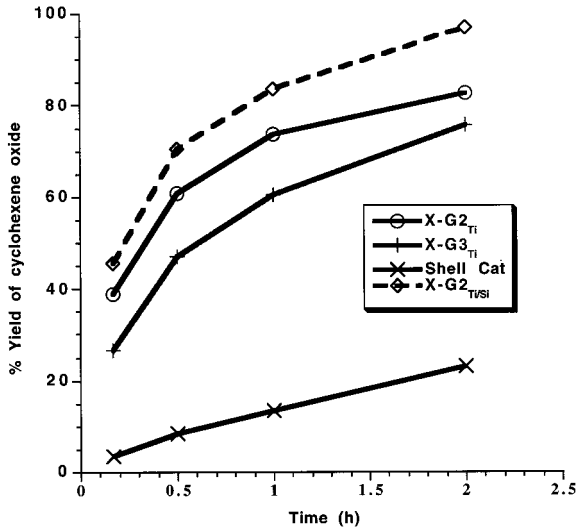

Figure 5. The yield of cyclohexene oxide in the catalytic epoxidation of cyclohexene using 0.025 g of **X-G2$_{Ti}$**, **X-G3$_{Ti}$**, the Shell catalyst, and **X-G2$_{Ti/Si}$**.

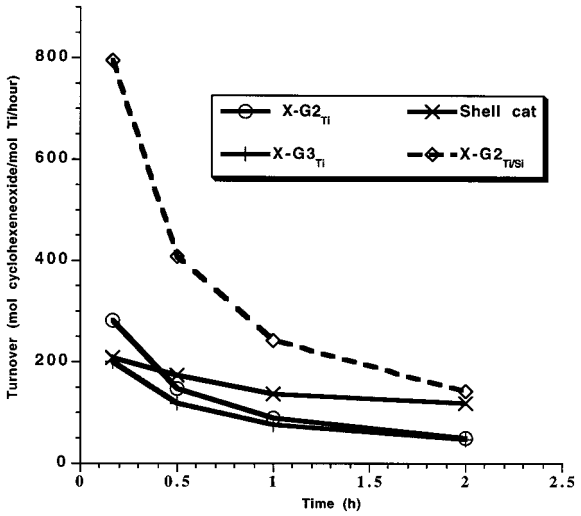

Figure 6. The turnover frequencies (TOF's) as a function of time during the epoxidation of cylclohexene using **X-G2$_{Ti}$**, **X-G3$_{Ti}$**, the Shell catalyst, and **X-G2$_{Ti/Si}$**.

The titanium-grafted gels were tested for catalytic activity in the epoxidation of cyclohexene using cumene hydroperoxide (CHP) as the oxidant. All three catalysts exhibited high conversion to cyclohexene oxide and 100% selectivity during the 2-h catalytic run. To assess the utility of **G2$_{Ti}$**, **X-G3$_{Ti}$**, and **X-G2$_{Ti/Si}$**, they were compared to the extensively studied Shell catalyst, prepared by treatment of partially dehydroxylated silica with Ti(O^{i}Pr)$_4$ and subsequent calcination at 600 °C in air.[28] The yield of cyclohexene oxide (based on the initial quantity of CHP) for the dendrimer-based xerogels was significantly higher than that for the Shell catalyst (Figure 5). Additionally, our Ti-supported, dendrimer-based gels compare well in activity with the Ti-grafted aerogels reported by Baiker et al.[27b] Moreover, to our knowledge **X-G2$_{Ti/Si}$** is the most active catalyst thus far reported in terms of % conversion to cyclohexene oxide. All three dendrimer-based gels compare favorably with the Shell catalyst in terms of turnover frequency TOF (mole of cyclohexene oxide per mole of Ti per hour) and the TOF for **X-G2$_{Ti/Si}$** was found to be particularly high (see Figure 6). Additionally, **X-G2$_{Ti}$** and **X-G2$_{Ti/Si}$** are significantly more active than the Shell catalyst at the early part of the catalytic reaction with the initial rates (in terms of cyclohexene oxide production) for **X-G2$_{Ti}$**, **X-G3$_{Ti}$**, **X-G2$_{Ti/Si}$**, and the Shell catalyst of 7.8, 5.3, 9.1, and 0.7 mmol min^{-1} (g cat)$^{-1}$, respectively.

Catalysts **X-G2$_{Ti}$**, **X-G3$_{Ti}$**, and **X-G2$_{Ti/Si}$** were tested for catalyst leaching by heating a toluene suspension of the catalyst for 1 h at 65 °C in the presence of CHP, and then filtering the mixture. The filtrate was then utilized under the same conditions as the other catalytic reactions, and no cyclohexene oxide formation was observed by GC analyses. Thus, no evidence for homogeneous catalysis was found.

Concluding Remarks

The synthesis of high surface area dendrimer-based xerogels, with surface areas as high as 1336 m^2/g, has been achieved by the hydrolysis of alkoxysilyl-terminated dendrimers in a nonpolar solvent. The relatively high surface areas of the materials reported here can, to a large extent, be attributed to the evaporation of nonpolar solvents from the wet gels. Accordingly, homogeneous monoliths were formed from hydrolysis of the **G2-(OEt)$_{36}$** and **G3-(OEt)$_{108}$** dendrimers in benzene solution. From these experiments, we have found that both the molecular structure and the number of alkoxysilyl end groups play a role in the gelation behavior. The formation of polymeric monoliths in these cases may be associated with their highly hydrophobic interior, which (despite their hydrophilic periphery) keeps them in solution during the condensation process. Conversely, only a relatively small proportion of TEOS, 4,4′-bis(triethoxysilyl)biphenyl, and **G1-(OEt)$_{12}$** are hydrophobic. Thus, the corresponding hydrolyzed species probably become insoluble in benzene solution during the polymerization process and precipitate out of solution.

The observed correlation between gelation time in benzene and dendritic generation suggests that the number of end groups is also an important factor in monolith formation. The alkoxysilyl dendrimers with 36 and 108 end groups form monoliths in 4.5 and 2 days, respectively, whereas the corresponding first generation dendrimer with 12 end groups does not form a monolith and gives a low surface area material. This observation is consistent with the Carothers equation, which states that the total number of bonds needed to form a gel is inversely proportional to the number of reactive groups on the monomer.[30] Hence, the total number of condensations required for **G3-(OEt)$_{108}$** is considerably less than that required for **G1-(OEt)$_{12}$** to reach the gelation point. Additionally, our findings suggest that the number of end groups per unit volume plays a role in the gelation process. Although hydrolyses of **G2-(OEt)$_{36}$** and **G3-(OEt)$_{108}$** in a variety of organic solvents leads to high surface area xerogels, dendrimers **G2-(OEt)$_{24}$Me$_{12}$** and **G3-(OEt)$_{72}$Me$_{36}$** under similar conditions gel much later and give nonporous products. Additionally, the latter dendrimers may produce polymerized materials

(29) Wulff, H. P.; Wattimena, F. (Shell Oil Co.) US Patent 4,021,-454, 1977.

(30) Odian, G. *Principles of Polymerization*; John Wiley and Sons: New York, 1991; Chapter 2.

with low structural rigidities, which cannot retain their porosities after desiccation of the wet gels.

Using nitrogen adsorption porosimetry, we found that **X-G3$_{benz}$** has a greater surface area than **X-G2$_{benz}$**. This finding is surprising in that silica particles typically exhibit a decrease in surface area with a concomitant increase in particle radii.[10] This observation may be rationalized on the basis of the assumption that second-generation dendrimeric building blocks compress onto one another more than the third-generation dendrimers comprising **X-G3$_{benz}$**. The greater flexibility of dendrimers of earlier generation[7a,31] probably explains this apparent compressibility in the gel products. The surface areas of the gels obtained in benzene solvent also increased dramatically by a washing protocol which presumably expels polar byproducts made from the sol−gel reaction, and thereby minimizes capillary forces and pore collapse during drying. On the basis of the nitrogen porosimetry data and SEM micrographs, these gels (**X-G2$_{HT}$** and **X-G3$_{HT}$**) have structural properties that resemble those for aerogel materials.

X-G2$_{HT}$ and **X-G3$_{HT}$** are intriguing catalyst supports for organometallic complexes due to their high surface areas and relatively isolated surface Si−OH sites. Of particular note is the aerogel-like material, **X-G2$_{HT}$**, which has a surface area of over 1300 m^2/g and a relatively low surface hydroxyl coverage of 3.0 OH/nm^2. Typical silica aerogels have relatively lower surface areas (Table 1) and higher surface hydroxyl coverages (5.0−5.7 OH/nm^2). Additionally, we determined that the hydrothermal stability of **X-G2$_{HT}$** is quite high (no appreciable change in surface area after heating in refluxing H_2O for 48 h was observed). In addition, the spectroscopically well-defined surface of these materials may allow new opportunities for the careful characterization of surface-bound species, which has proven difficult for silica-supported analogues.

In this study, we have demonstrated that **X-G2$_{HT}$** and **X-G3$_{HT}$** are highly effective catalyst supports for the Ti centers introduced with Ti(O^{i}Pr)$_4$ or Ti[OSi(O^{t}Bu)$_3$]$_4$. As shown in Figure 5, the supported organometallic complexes were found to be moderate to highly active in the epoxidation of cyclohexene, especially relative to the Shell catalyst. This is probably due, in part, to their relatively high surface areas and large pore volumes. Moreover, the tris(*tert*-butoxy)siloxide precursor supported on **X-G2$_{HT}$** (**X-G2$_{Ti/Si}$**) is remarkably active, both in terms of cyclohexene oxide yield and TOF. Apparently, the −OSi(O^{t}Bu)$_3$ ligands in **X-G2$_{Ti/Si}$** play an integral role in producing more active catalytic Ti sites. We propose that the alkoxy(siloxy) ligand environment of Ti[OSi(O^{t}Bu)$_3$]$_4$ facilitates the introduction of single-site −O−Ti(O−SiO$_3$) centers, which are thought to be most active in epoxidation catalysis.[32]

In conclusion, this work suggests that dendrimer-based xerogels are promising supports for catalytically active species. Future reports will address the design and synthesis of a wider range of materials of this type, and their use as catalyst supports.

(31) Frey, H.; Lach, C.; Lorenz, K. *Adv. Mater.* **1998**, *10*, 279.
(32) Bouh, A. O.; Rice, G. L.; Scott, S. L. *J. Am. Chem. Soc.* **1999**, *121*, 1, 7201.
(33) Brinker, C. J.; Scherer, G. W. *J. Non-Cryst. Solids* **1985**, *70*, 301.

Experimental Section

General. All reactions were performed under an inert dinitrogen atmosphere using standard Schlenk techniques. Tetrahydrofuran and hexanes were distilled from purple sodium−benzophenone ketyl and benzene and toluene were distilled from potassium metal. Chloroplatinic acid was purchased from Strem Chemical Company and used as a 0.1 M solution in dry 2-propanol. Triethoxysilane and methyldiethoxysilane were obtained from Gelest Inc. and distilled under nitrogen before use. The Ti(O^{i}Pr)$_4$ was obtained from Aldrich, distilled prior to use, and stored under a dinitrogen atmosphere. The Ti[OSi(O^{t}Bu)$_3$]$_4$ was prepared according to a literature procedure.[27d] The alkoxysilyl-terminated dendrimers **G2-(OEt)$_{36}$** and **G3-(OEt)$_{108}$** were prepared according to the procedure described in a previous publication.[7a] The analogous dendrimers, **G2-(OEt)$_{24}$Me$_{12}$** and **G3-(OEt)$_{72}$Me$_{36}$**, were prepared in identical fashion, except that HSiMe(OEt)$_2$ was used as the silane. The hydrolyses of these species was conducted in the specified solvent at a concentration of 2.5 M in Si−OEt groups. Freshly prepared 1 N HCl was used for all hydrolyses. The BET porosimetry data was collected on a Micromeritics ASAP 2010 instrument using either a 60-point or 80-point analysis. The ^{29}Si CP MAS NMR was collected on a Bruker AMX-400 MHz instrument and the peaks were deconvoluted using a Lorentz Gaussian (50:50) fit. Infrared spectra were recorded on a Perkin-Elmer 1330 infrared spectrometer as Nujol mulls on KBr plates (unless otherwise noted) and all absorptions are reported in centimeter^{-1}. Elemental analyses were performed by Mikroanalytisches Labor Pascher. The SEM micrographs were taken on a JEOL 35 CF and the samples were coated with 20 nm of Au/Pd alloy. TEM micrographs were taken on a JEOL 200cx at either 160 or 200 kV by depositing a pentane suspension of the finely ground gel on a "Type A" carbon coated Cu grid obtained from Ted Pella Inc.

X-G3$_{THF}$. To a freshly prepared sample of **G3-(OEt)$_{108}$** (0.094 mmol) was added 4.1 mL of fresh (dry) THF. The resulting **G3-(OEt)$_{108}$** solution was transferred via filter cannula to a Schlenk tube. Subsequently, 0.20 mL of a 1.0 N HCl solution was added to the reaction mixture which was then stirred for 5 min at room temperature. The homogeneous sol solution was transferred to a 25-mL polyethylene (PE) bottle via cannula and quickly capped. After at least 5 days, the resulting clear monolith was removed from the PE bottle intact and solvent-processed as described in ref 16. The gel was then allowed to dry at room temperature for at least 3 days during which time it shrunk considerably and cracked into several pieces. The xerogel **X-G3$_{THF}$** was ground to a fine powder and placed under dynamic vacuum at 100 °C for 24 h. ^{29}Si CP MAS NMR (39.73 MHz): δ 6.0 (br), −46.2 (T^1), −56.0 (T^2), −64.9 (T^3). IR (KBr): 3450 (br), 2915, 1463, 1261, 1086, 1030, 904, 792.

X-G2$_{THF}$. A procedure similar to that used in the synthesis of **X-G3$_{THF}$** was employed. ^{29}Si CP MAS NMR (39.73 MHz): δ 7.0 (br), −46.2 (T^1), −55.0 (T^2), −63.9 (T^3). IR (KBr): 3439 (br), 2915, 1463, 1261, 1082, 1030, 902, 790.

X-G2$_{benz}$. A hydrolysis protocol similar to that used in the synthesis of **X-G3$_{THF}$** was employed, except that dry distilled benzene was used as the solvent. A

monolithic gel was obtained after ~4 days and was allowed to further age for at least another 3 days. The wet gel was solvent-processed by washing with copious amounts of C_6H_6 in a fine fritted funnel. The gel was then air-dried and dried under dynamic vacuum as in the synthesis of **X-G3$_{THF}$**. ^{29}Si CP MAS NMR (39.73 MHz): δ 6.1 (br), −47.1 (T^1), −56.0 (T^2), −64.8 (T^3). IR: 3447 (br), 2985, 1461, 1262, 1079, 1037, 896, 772.

X-G3$_{benz}$. The synthetic protocol was identical to that used for the synthesis of **X-G3$_{benz}$**. ^{29}Si CP MAS NMR (39.73 MHz): δ 6.1 (br), −47.1 (T^1), −56.0 (T^2), −64.8 (T^3). IR: 3445 (br), 2923, 1460, 1262, 1077, 1028, 895, 772.

X-G2$_{HT}$. The synthetic protocol was identical to that used for **X-G2$_{benz}$**, except that after aging of the wet gel, it was heated in toluene at ~100 °C for 48 h. The gel was then isolated as a fine powder, washed with copious amounts of fresh toluene, air-dried for ~3 days, and dried under dynamic vacuum, after which time a fluffy off-white powder was obtained. ^{29}Si CP MAS NMR (39.73 MHz): δ 7.6 (br), −46.8 (T^1), −55.8 (T^2), −64.6 (T^3). IR: 3419 (br), 2926, 1462, 1260, 1080 (br), 902, 788.

X-G3$_{HT}$. The synthetic protocol was identical to that used for the synthesis of **X-G2$_{HT}$**. ^{29}Si CP MAS NMR (39.73 MHz): δ 6.5 (br), −45.3 (T^1), −54.9 (T^2), −64.8 (T^3). IR: 3443, 2944, 1457, 1258, 1019 (br), 894, 783.

X-G2$_{Ti}$. To a 50-mL two-necked round-bottom flask equipped with a reflux condenser and nitrogen inlet valve was added 0.316 g of **X-G2$_{HT}$**, excess Ti(O^{i}Pr)$_4$ (2.08 g) and ~20 mL toluene. This solution was heated at reflux for 48 h. The solvent was removed in vacuo, and the solid residue was washed with copious amounts of toluene and hexanes. The off-white powder was dried under dynamic vacuum for 12 h at 100 °C and subsequently stored in a dinitrogen filled drybox. ^{29}Si CP MAS NMR (39.73 MHz): δ 6.1 (br), −57.9 (T^2), −65.8 (T^3). IR: 3330 (br), 2923, 1462, 1258, 1127 (br), 1009 (br), 778. Anal. Found: Ti, 7.91%.

X-G3$_{Ti}$. A procedure similar to that used for the synthesis of **X-G2$_{Ti}$** was employed. ^{29}Si CP MAS NMR (39.73 MHz): δ 7.8 (br), −56.7 (T^2), −64.3 (T^3). IR: 3421 (br), 2930, 1462, 1124, 1013 (br), 854, 722. Anal. Found: Ti, 7.61%

X-G2$_{Ti/Si}$. A toluene solution of Ti[OSi(O^{t}Bu)$_3$]$_4$ (0.611 g, 5.55 mmol) was heated at reflux in the presence of 0.100 g of **X-G2$_{HT}$**. The product was isolated by following an identical procedure to that used for **X-G2$_{Ti}$**. ^{29}Si CP MAS NMR (39.73 MHz): δ 7.4, −55.6 (T^2), −62.5 (T^3) −100.5 (br) (siloxide). IR: 3422 (br), 2940, 1366, 1243, 1071, 1029, 929, 789, 722. Anal. Found: Ti, 3.27%.

X$_{TEOS}$. To a Schlenk flask containing 10.25 mL of dry C_6H_6 was added 2.0 mL of TEOS followed by 0.71 mL (4.4 equiv) of a freshly prepared solution of 1 N HCl. This solution was stirred at room temperature for 20 min and subsequently transferred to a PE bottle and capped. Over ~6 days, a brittle white solid precipitated out of solution. A monolith was not formed. The solid was isolated by filtration and washed with copious amounts of C_6H_6, air-dried for 2 days, and placed under high vacuum at 100 °C overnight. ^{29}Si CP MAS NMR (39.73 MHz): δ −92.1 (Q^2, 12.5%), −101.3 (Q^3, 73.7%), −110.8 (Q^4, 13.8%). IR: 3406 (br), 1165, 1075 (br), 919, 799, 572.

X$_{biphen}$. The 4,4′-bis(triethoxysilyl)biphenyl was prepared according to a literature procedure.[16] The silylalkoxy species (0.85 g, 1.78 mmol) was added to a Schlenk tube and subsequently diluted with 4.3 mL of C_6H_6 and 0.21 mL of 1 N HCl. This solution was stirred at room temperature for 20 min and then transferred to a PE bottle and capped. Over ~21 days, a dense particulate material precipitated out of solution. A monolith was not formed.

Hydrolysis of G1-(OEt)$_{12}$. This precursor was made by a procedure similar to that used for the synthesis of **G3-(OEt)$_{108}$.** However, in this case the starting material was tetravinylsilane obtained from Gelest Inc. Hydrolysis of **G1-(OEt)$_{12}$** in C_6H_6 was conducted by following an identical protocol as that used for **X-G2$_{benz}$** and **X-G3$_{benz}$**. BET analysis of the isolated xerogel showed no appreciable surface area.

X-G2Me and X-G3Me. These xerogels were made by hydrolysis of **G2-(OEt)$_{24}$Me$_{12}$** and **G3-(OEt)$_{72}$Me$_{36}$**, respectively, using protocols identical to those employed for **X-G2$_{benz}$** and **X-G2$_{THF}$**. All four xerogels (**X-G2Me$_{THF}$**, **X-G3Me$_{THF}$**, **X-G2Me$_{benz}$**, and **X-G3Me$_{benz}$**) had no appreciable surface area, as determined by BET analysis.

Gel Functionalization. The following general procedure was used. A J-Young type NMR tube was charged with a deuterated NMR solvent (benzene-d_6 for the chlorosilanes and toluene-d_8 for Ti(O^{i}Pr)$_4$) and carefully weighed out amounts of ferrocene and a chlorosilane or Ti(O^{i}Pr)$_4$ (see Table 3). A ^{1}H NMR spectrum was then acquired using one scan. A carefully weighed out sample of either **X-G2$_{HT}$** or **X-G3$_{HT}$** was then added to the NMR tube. The NMR tube reactions were then heated at the boiling point of the solvent and monitored periodically by ^{1}H NMR spectroscopy until consumption of the soluble reagent was no longer evident (~24−48 h).

Catalysis Procedure. Epoxidation reactions were conducted under N_2 at 65 °C using 0.025 g of catalyst, 1.0 mL of cyclohexene, 0.92 mL of cumene hydroperoxide, 0.25 mL of dodecane, and 5 mL of toluene. Aliquots were removed and filtered for GC analysis 0, 10, 30, 60, and 120 min after cumene hydroperoxide injection.

Acknowledgment. This work was supported by the Director, Office of Energy Research, Office of Basic Energy Sciences, Chemical Sciences Division, of the U. S. Department of Energy under Contract No. DE-AC03-76SF00098. We are grateful to Drs. R. Gronsky, C. Lugmair, and M. Coles for helpful discussions, and to Professors E. Iglesia and J. M. J. Frechet for generous use of their BET instruments. Dr. Martyn Coles is also acknowledged for a generous supply of Ti[OSi(O^{t}Bu)$_3$]$_4$.

CM000098G